ISSN 1674-1056
http://cpb.iphy.ac.cn
http://iopscience.iop.org/cpb
中国物理 B
Chinese Physics
中国物理 Chinese Physics B

Experimental demonstration of narrow-band rugate minus filters using rapidly alternating deposition technology

Ying Zhang(章瑛), Yan-Zhi Wang(王胭脂), Jiao-Lin Zhao(赵娇玲), Jian-Da Shao(邵建达), Shuang-Chen Ruan(阮双琛)
Citation: Chin. Phys. B . 2018, 27(5): 054208. **doi:** 10.1088/1674-1056/27/5/054207

Journal homepage: http://cpb.iphy.ac.cn; http://iopscience.iop.org/cpb

What follows is a list of articles you may be interested in

Photonic crystal fiber polarization filter with two large apertures coated with gold layers

Jun-Jun Wu(吴君君), Shu-Guang Li(李曙光), Qiang Liu(刘强), Min Shi(石敏)
Chin. Phys. B . 2017, 26(11): 114209. **doi:** 10.1088/1674-1056/26/11/114209

Mechanically tunable metamaterials terahertz dual-band bandstop filter

Fangrong Hu(胡放荣), Xin Xu(胥欣), Peng Li(李鹏), Xinlong Xu(徐新龙), Yue'e Wang(王月娥)
Chin. Phys. B . 2017, 26(7): 074219. **doi:** 10.1088/1674-1056/26/7/074219

Tunable optical filter using second-order micro-ring resonator

Lin Deng(邓林), Dezhao Li(李德钊), Zilong Liu(刘子龙), Yinghao Meng(孟英昊), Xiaonan Guo(郭小男), Yonghui Tian(田永辉)
Chin. Phys. B . 2017, 26(2): 024209. **doi:** 10.1088/1674-1056/26/2/024209

Analysis of the spatial filter of a dielectric multilayer film reflective cutoff filter-combination device

Zhang Ying, Qi Hong-Ji, Yi Kui, Wang Yan-Zhi, Sui Zhan, Shao Jian-Da
Chin. Phys. B . 2015, 24(10): 104216. **doi:** 10.1088/1674-1056/24/10/104216

An improved transmitting multi-layer thin-film filter

Zhang Ying, Qi Hong-Ji, Yi Kui, Wang Yan-Zhi, Sui Zhan, Shao Jian-Da
Chin. Phys. B . 2015, 24(5): 054212. **doi:** 10.1088/1674-1056/24/5/054212

Modulation and mechanism of ultrafast transient spectroscopy based on dimethylamino-carbaldehyde derivatives*

Tong-xing Jin(金桐兴)[1], Jun-yi Yang(杨俊义)[1], Yu Fang(方宇)[2], Yan-bing Han(韩艳兵)[3], and Ying-lin Song(宋瑛林)[1,3,†]

[1] College of Physics, Optoelectronics and Energy, Soochow University, Suzhou 215006, China
[2] Jiangsu Key Laboratory of Micro and Nano Heat Fluid Flow Technology and Energy Application, School of Mathematics and Physics, Suzhou University of Science and Technology, Suzhou 215009, China
[3] Department of Physics, Harbin Institute of Technology, Harbin 150001, China

(Received 28 September 2017; revised manuscript received 30 January 2018; published online 26 April 2018)

Two dimethylamino-carbaldehyde derivatives with different π-bridge lengths were prepared, and their transient optical properties and photophysical mechanisms were investigated by transient absorption spectroscopy and Z-scan measurements. Owing to the difference in molecular structures, the two compounds exhibit different populations of locally excited states and, therefore, they also produce different transient absorption spectra. After photoexcitation, both molecular materials exhibit a wide excited state absorption band from 450 nm to 1000 nm. Meanwhile, the excited state lifetimes are dramatically different, 2 ns and 100 ps, for the two molecules. A figure of merit greater than 2 at the wavelength of 1000 nm is obtained. The results show that modulating the population of the locally excited states in this type of molecule can be a promising approach for obtaining optical switching and solar cell materials.

Keywords: nonlinear optics, transient absorption spectra, dimethylamino-carbaldehyde derivatives

PACS: 42.50.Md, 78.47.jb, 42.70.Nq **DOI:** 10.1088/1674-1056/27/5/054208

1. Introduction

Nonlinear optical (NLO) materials have many potential uses in various photoelectronic devices and photonic applications.[1–3] Much effort has been devoted to the development of NLO devices with a large nonlinear response.[4–6] Accompanied by the advance of materials chemistry, researchers are no longer satisfied with optical nonlinearity at specific wavelengths, and broadband response becomes a desired property in developing nonlinear optical materials. Donor-π-acceptor (D-π-A) molecular materials have recently attracted considerable academic and technological research attention for their applications in nonlinear optics.[7–9] Their NLO properties can be adjusted by the appropriate manipulation of their chemical structures such as the different connectors linking the electron-donor/electron-acceptor (D/A) building blocks, the distance between the D/A units, and the symmetry of the molecular structure.[10–12] Many types of functional groups with strong electron withdrawing or electron donating properties, linked to a connector, have been selected by researchers for study. Although this is a good approach for synthesizing materials with large NLO properties and broadband response, the results have not always been satisfactory.

Transient absorption spectroscopy is widely used to follow photophysical dynamics in molecular systems.[13–15] In the field of nonlinear optics, transient absorption spectra are widely used in studying the NLO properties of materials.[16–18] Modulating the transient absorption spectra of materials can lead to broadband excited state absorption and enhanced NLO properties. For many fluorescent materials with D-π-A structure, two excited states, namely, locally excited (LE) states and intramolecular charge-transfer (ICT) states, are accessible upon photoexcitation. The LE states are proposed to be emissive, but the ICT states are usually not.[19–21] Suppressing transition from the LE states to the ICT states results in increased population of the LE states, and thus, the fluorescence emission intensity will be enhanced.[22,23] However, the transient absorption spectra of these materials can also exhibit saturated absorption (SA) due to the influence of the stimulated emission. Our interest is in modulating the transient absorption spectra of D-π-A molecular materials by changing the population of the LE states. This approach has been used to obtain improved fluorescent materials, but there are few reports on modulating the transient absorption spectra of materials in this way.

Herein, we report investigations into two dimethylamino-carbaldehyde derivatives 4-{2-[4-(N,N-dimethylamino)phenyl]ethynyl} benzenecarbaldehyde (DPC) and 4'-(dimethylamino)-[1,1'-biphenyl]-4-carbaldehyde (DBC). Owing to the difference of molecular structures, upon photoexcitation, tilted molecules exhibit different population of locally excited (LE) states. In order to study the influence of tuning the population of the LE states on transient absorption

*Project supported by the National Natural Science Foundation of China (Grant Nos. U1630103 and 11704273), Natural Science Foundation of Jiangsu Province, China (Grant No. BK20170375), and Natural Science Foundation of the Higher Education Institutions of Jiangsu Province, China (Grant No. 17KJB140021).

†Corresponding author. E-mail: ylsong@hit.edu.cn

© 2018 Chinese Physical Society and IOP Publishing Ltd

spectra and NLO properties, we systematically investigate the broadband nonlinear optical properties of DPC and DBC by performing broadband transient absorption spectroscopy and *Z*-scan measurements with 190 fs laser pulses. Our results demonstrate that tuning the population of the LE states of this type of material can enhance its NLO properties, and we conclude that such methods may be considered as a promising candidate for modulating their transient absorption spectra.

2. Experimental measurements

2.1. Materials and quantum chemical calculations

The first compound, DPC, is a diphenylacetylene derivative with a dimethylamino group and a carbaldehyde group, and the second, DBC, is a biphenyl derivative with the same groups (Fig. 1). The synthesis of DPC and DBC has been described in detail elsewhere.[24,25] Both these compounds can be obtained from commercial chemical suppliers. They have the same electron-donor and electron-acceptor but different π-bridge lengths. In this case, the ethyne link in DPC, as the longer π-bridge, provides more extended π-conjugation along the direction of the π-bridge. Therefore, DPC has better charge transfer capability.[26,27]

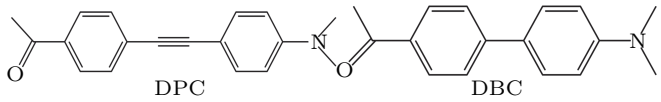


Fig. 1. Molecular structures of the asymmetric dimethylamino-carbaldehyde derivatives DPC and DBC.

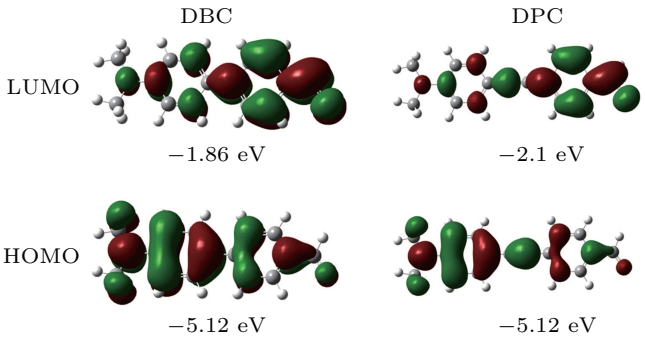


Fig. 2. (color online) Frontier molecular orbital distributions and their energies of DBC and DPC.

In order to study the relationship between the structures and the properties of the compounds, density functional theory (DFT) calculations were performed using Gaussian 09 software.[28] A B3LYP/6-31G(d,p)//CPCM (DMSO) model was used to optimize the structures of the molecular systems. The electron-cloud distribution of various frontier molecular orbitals was estimated from these calculations, and the results are summarized in Fig. 2. In general, the electron in the highest occupied molecular orbit (HOMO) is excited to the lowest unoccupied molecular orbit (LUMO) after photoexcitation. For the two molecules in our study, the dimethylamino group serves as the electron donor and the carbaldehyde group as the electron acceptor. Both molecules have the same functional groups. The energy band gaps of DPC and DBC are 3.02 eV and 3.26 eV, respectively. We found that the HOMO–LUMO gap of DPC is induced by relatively stronger intramolecular charge transfer, and as a result, its absorption band can extend toward longer wavelengths.[29,30]

2.2. Transient absorption spectroscopy

Broadband transient absorption measurements were performed using femtosecond pulses generated by a regeneratively amplified Yb: KGW fiber laser system (Light Conversion, PHAROSSP) that produces pulses with energies of 1 mJ, centered at 1030 nm, with a repetition rate of 6 kHz, and a full width at half maximum (FWHM) of 190 fs. The main portion of the output was delivered to pump an optical parametric amplifier (OPA, ORPHEUS, Light Conversion). The OPA output was tuned to a wavelength of 365 nm, and this was used as the pump beam for the transient absorption excitation. Before interacting with the sample, this beam was modulated at 137 Hz using a chopper, and attenuated to the desired intensity using a gradual neutral density optical filter for minimizing undesired cross-phase modulation effects. Probe pulses for spectroscopic characterization were produced by passing a small portion of the laser output at 1030 nm wavelength through a computer-controlled optical delay stage (with a maximum delay line of 1830 ps) and focusing it onto a 2-mm-thick Ti:sapphire plate to produce a white-light continuum spanning the 455–1000 nm window. The polarization of the pump and the probe pulses at the sample location was at the magic angle to avoid the anisotropic effect. The angle between the pump and the probe beams was 5° and the beam waists of the pump and probe beams were 1 mm and 100 μm, respectively, in the sample solution.

2.3. *Z*-scan measurements

The NLO properties of the two asymmetric dimethylamino-carbaldehyde derivatives were measured using the *Z*-scan technique. The light source for the femtosecond *Z*-scan was an OPA (ORPHEUS, 190 fs, 20 Hz, Light Conversion) with a tunable output wavelength ranging from 760 nm to 1000 nm. The experimental apparatus has been described in detail elsewhere.[31] The sample solution was injected into 2-mm-thick cuvettes. The cell was placed on a translation stage manipulated by a computer that moved along the *Z*-axis of the focal point of a lens with a 400-mm focal length. The laser pulses, after modulation by an attenuator, were separated into two beams by using a beamsplitter; one beam was focused on the sample through a lens with a 400-mm focal length and the other beam served as the reference beam. The two beams were

simultaneously measured using two energy detectors (Rjp-765 Energy Probe, Laser Probe, Inc.) linked to an energy meter (Rj-7620 Energy Ratiometer, Laser Probe, Inc.). A computer was used to collect the data from the energy meter through a general-purpose interface bus (GPIB). All of the samples were measured using dimethylsulfoxide (DMSO) as the solvent.

3. Results and discussion

3.1. UV–Vis absorption and fluorescence spectra

The ultraviolet–visible (UV–Vis) absorption spectra of the compounds DBC and DPC were recorded in a diluted DMSO solution (1×10^{-5} mol/L) at room temperature, and the results are presented in Fig. 3. The absorption and fluorescence spectra of the solvent (dilute DMSO) are also presented in Fig. 3, and it is apparent that the influence of the solvent on the fluorescence spectra of DBC and DPC is negligible. The maximum absorption bands of DPC and DBC are located at 390 nm and 374 nm, respectively. The absorption band-edges of DPC and DBC are at 470 nm and 448 nm, respectively. Based on the maximum absorption bands, the energy band gaps of DPC and DBC are 3.18 eV and 3.32 eV, respectively. These results are in agreement with the quantum chemical calculation results. It should be noted that DPC exhibits red-shifted absorption because it has a longer π-bridge length than DBC. DBC shows a strong fluorescent signal centered at 545 nm, while the fluorescent signal of DPC could not be observed. DPC, with the more extended conjugation length exhibits better intramolecular charge transfer capacity, which is beneficial for enhancing the transition from the LE states to the ICT states. As a result, the population of the LE states is suppressed and the fluorescence emission intensity is quenched.[32] Our results demonstrate that tilted molecules exhibit different populations of LE states. In order to study the influence of the modulation on transient absorption spectra and NLO properties, we designed and implemented transient absorption spectra and Z-scan experiments.

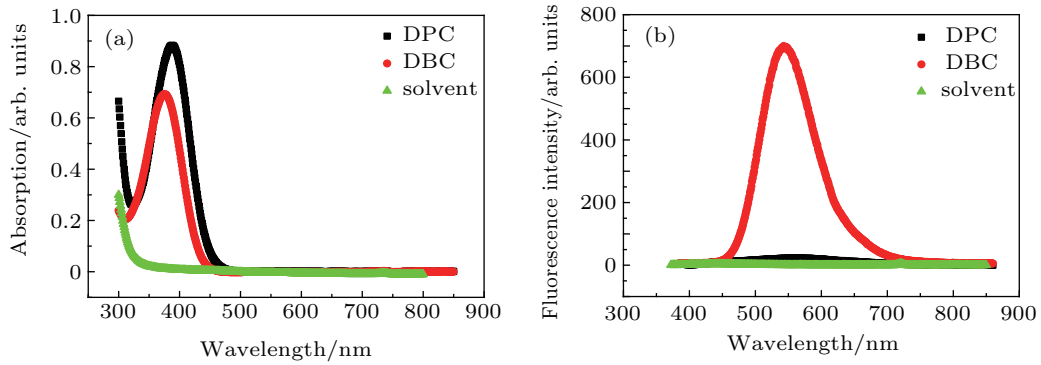


Fig. 3. (color online) (a) UV–Vis absorption and (b) fluorescence emission spectra of DPC and DBC in a diluted DMSO solution.

3.2. Transient absorption spectroscopy

The femtosecond transient absorption spectra were recorded separately in the visible light region and the near-infrared band with 190 fs laser pulses as the pump at the wavelength of 365 nm; the spectra are plotted in Fig. 4. DBC and DPC were dissolved in DMSO, with concentrations 0.02 mol/L and 0.018 mol/L, respectively. The transient absorption measurement shows positive and negative signals as a function of the delay time and wavelengths, which correspond to reverse saturated absorption (RSA) and saturated absorption (SA) effects, respectively. The fluorescence emission spectra of the samples demonstrate that the population of the LE states of DBC is obviously larger than that of DPC upon photoexcitation. The transient absorption spectra of the samples exhibit different responses as well. In Fig. 4(c), the valley of negative signal of DBC exhibits a redshift from 520 nm to 540 nm. Then, the valley of negative signal is 550 nm. The behavior indicates the existence of many higher-lying vibronic levels of the LE states. Under photoexcitation, the molecules are excited to the higher-lying vibronic levels of the LE states and then return to the lowest vibronic level of the LE states (S_{LE1}). The valley of the negative signal is 550 nm in S_{LE1} state, which is the same as the center of the fluorescence signal. As a result, the stimulated emission center of the LE states of DBC is 550 nm and the negative signal of DBC occurring in the visible region between 470 nm and 670 nm is ascribed to the stimulated emission (see fluorescence spectra in Fig. 3(b)). Figure 4(a) indicates an obvious change on the transient absorption spectra of DPC. Through the same theoretical analysis, the absorption peak of the LE states of DPC is 490 nm. Owing to the stimulated emission from the LE states of DPC, the negative signal occurs in the visible region between 540 nm and 690 nm. The negative signal has a short lifetime (4 ps) and weaker signal intensity. After 4 ps, the charge transfers from the LE states to the ICT states and the response becomes a positive signal. The findings are ascribed to the absorption of the ICT states and the absorption peak is 627 nm. The transient absorption spectrum of DPC exhibits

a broadband RSA range from the visible to the near-infrared region (see Figs. 4(a) and 4(b)). Moreover, the modulation also enhances the RSA of the samples. Though the transient absorption spectrum of DBC exhibits positive signal between 680 nm and 1000 nm (see Fig. 4(b)), the response of DBC is weaker than that of DPC. Comparing Figs. 4(b) and 4(d), we note that although the signal of DBC approaching longer wavelengths near 1000 nm obviously drops, the RSA of DPC may extend even further into the near-infrared region because there is no clear decline in RSA at 1000 nm. Owing to the response limitation of the silicon detector, the probe wavelength can only reach 1000 nm in our experiment.

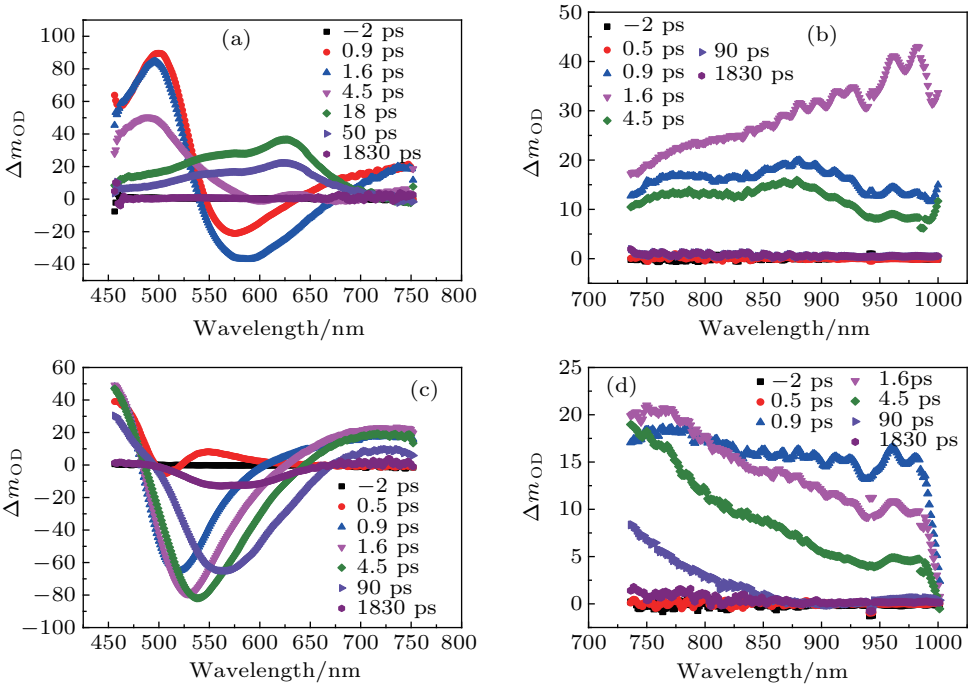


Fig. 4. (color online) Transient absorption spectra of DPC and DBC pumped at 365 nm with 190 fs laser pulses. (a) and (b) The visible light and near-infrared transient absorption spectra of DPC, respectively. (c) and (d) The visible light and near-infrared transient absorption spectra of DBC, respectively.

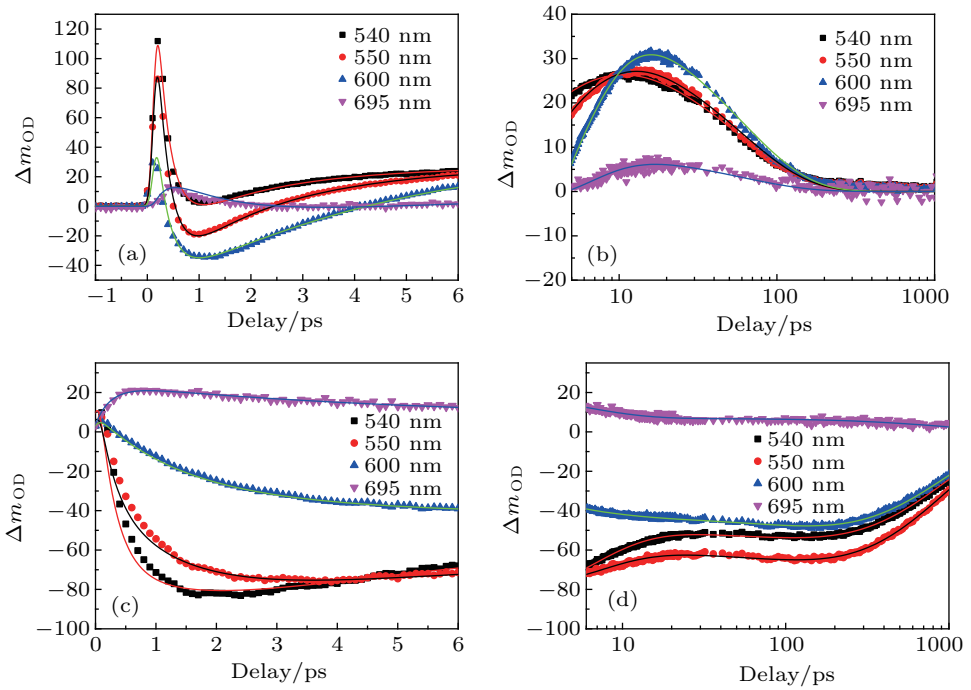


Fig. 5. (color online) Time-response curves of DPC and DBC: (a) the short-delay time curves of DPC from 0 ps to 6 ps, (b) the long-delay time curves of DPC from 6 ps to 1000 ps, (c) the short-delay time curves of DBC from 0 ps to 6 ps, (d) the long-delay time curves of DBC from 6 ps to 1000 ps. The colored circles represent the experimental data and the corresponding colored solid lines represent theoretical fitting.

Table 1. Excited state lifetime of DPC and DBC.

Parameters	τ_0/ps	τ_1/ps	τ_2/ps	τ_3/ps
DPC	0.24	4	1.5	60
DBC	6	0.002	–	–

In order to study the dynamic process of the two compounds, the time-resolved transient absorptions of DBC and DPC are displayed in Figs. 5(a)–5(d). Figure 5(a) indicates that the negative signal occurs in the visible region from 0.2 ps to 4 ps, which corresponds to the LE states of DPC. Then, the response becomes a positive signal, which corresponds to the ICT states. In Fig. 5(c), the negative signal occurs in the visible region from 0 ps to 1000 ps, which corresponds to the LE states of DBC. From these experimental results, the energy-level models of the samples may be established. Through global analysis, the excited states lifetime of DPC and DBC can be obtained (see Table 1). The theoretical fitting curves of the dynamic process are consistent with the experimental data (see Fig. 5). There are many higher-lying vibronic levels of the LE states and ICT states. Figures 6(a) and 6(b) are the simplified energy level diagrams of DPC and DBC. S_{LE1} and S_{LE2} belong to the LE states: S_{LE1} is the lowest vibronic level of the LE states and S_{LE2} is the equivalent high energy level of the LE states. S_{ICT1} is the equivalent high level of the ICT states and S_{ICT2} is the lowest vibronic level of the ICT states. The photodynamics of DPC is shown in Fig. 6(a). Under photoexcitation, the molecules in their ground state S_0 are excited to S_{LE2} and then relax to S_{LE1} through vibrational cooling relaxation (VCR), this process lasts 0.24 ps. Next, the molecules transfer to the ICT states (S_{ICT1}) and then relax to the S_{ICT2} state; these two processes take place after 4 ps and 1.4 ps. Finally, the molecules return to the ground state; this process has a lifetime of about 60 ps. Figure 6(b) exhibits the dynamic process of DBC, after photoexcitation; molecules from the ground state S_0 are excited to S_{LE2}. Then, the molecules relax to S_{LE1} via vibrational cooling relaxation. Finally, the molecules fluoresce as they return to S_0.

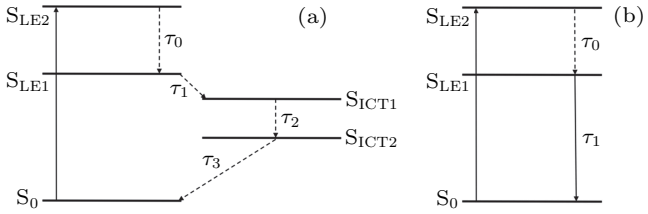


Fig. 6. Simplified energy-level model of (a) DPC and (b) DBC. The dotted lines represent non-radiative transitions, and the solid line represent radiative transitions.

3.3. *Z*-scan measurements

The transient absorption spectroscopy results demonstrate that the modulation can enhance RSA in the near-infrared band. With the aim of evaluating the influence of our modulation on nonlinear coefficients in the near-infrared band, open-aperture and closed-aperture *Z*-scan measurements with femtosecond laser pulses were conducted at different wavelengths. DBC and DPC were dissolved in DMSO using the same concentrations as in the transient absorption spectroscopy. The solvent itself did not exhibit any nonlinear absorption under our experimental conditions. We presumed that two-photon absorption (TPA) dominated the nonlinear mechanism on the femtosecond time scale because the molecules we were studying did not show any linear absorption in the near-infrared region (Fig. 3). Therefore, we selected 760-nm open-aperture *Z*-scan measurements of DPC and DBC to verify our conjecture. The *Z*-scan curves at 760 nm for different input intensities are shown in Fig. 7. Through theoretical fitting, we calculated the effective nonlinear absorption coefficient β_{eff} at different levels of laser intensity I. The β_{eff} values of DPC and DBC did not change with an increase in I (Table 2). The result is consistent with our assumption.

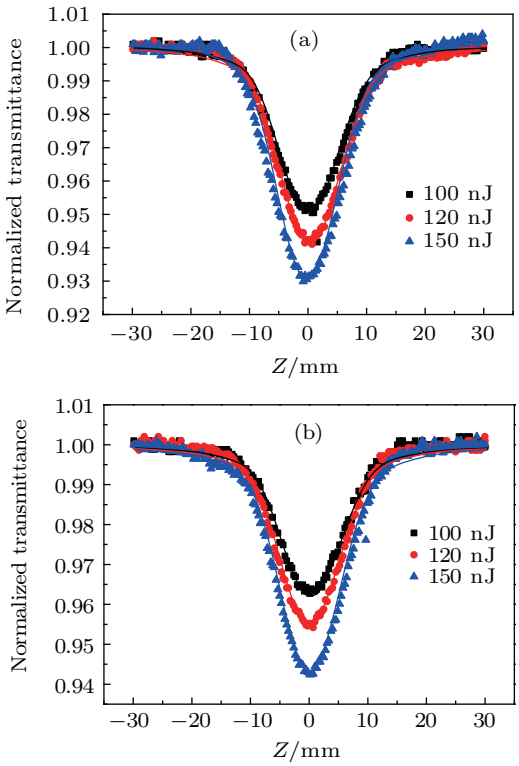


Fig. 7. (color online) Example of open-aperture *Z*-scan of (a) DPC and (b) DBC at input intensities of 100 nJ, 120 nJ, and 150 nJ at 760 nm. The colored circles represent the experimental data and the corresponding colored solid lines represent the theoretical fitting.

Table 2. TPA coefficients β_{eff} for DPC and DBC at different levels of light intensity I at 760 nm.

I/nJ	$\beta_{\text{eff}}/10^{-2}$ cm·GW^{-1}	
	DPC	DBC
100	4.2	3.1
120	4.1	3.0
150	4.1	3.1

Furthermore, we observed TPA and the third-order Kerr refraction nonlinearities caused by TPA using Z-scan experiments at wavelengths ranging from 760 nm to 1000 nm (Fig. S1, supporting information). The DMSO solvent has a nonlinear refraction. To avoid the influence of the solvent, the nonlinear refraction of the solvent was eliminated and thereby we obtained the nonlinear refraction of the pure sample. Through theoretical fitting, the values of the effective nonlinear absorption coefficient (β_{eff}) and the nonlinear refractive index (n_2) were calculated. The nonlinear figures of merit ($f = n_2/(\beta_{\text{eff}} \cdot \lambda)$)[33] of DPC and DBC were also calculated. The values are listed in Table 3.

Table 3 shows that DPC and DBC exhibit TPA and Kerr refraction at each wavelength of photoexcitation. TPA is strongest at 800 nm for DBC and DPC. The TPA coefficients of both DPC and DBC decrease rapidly, while the nonlinear refractive index decreases very slowly, as the wavelength gets longer. The figures of merit of DBC and DPC show an increasing trend from 760 nm to 1000 nm. We observe that DPC has larger optical nonlinearity and a higher figure of merit than DBC at the same wavelength. Furthermore, DPC exhibits a wider absorption band than DBC. These results demonstrate that our modulation can also enhance the NLO properties of the molecules. The figure of merit of DPC is greater than 2 at 1000 nm and the value may be even larger at longer wavelengths, making it a potential candidate for applications in communication bands. The figure of merit is an important parameter for optical-switching materials. A high nonlinear refractive index indicates that the material exhibits good switching performance and low nonlinear absorption, which translates into low light intensity requirements.

Table 3. TPA coefficients (β_{eff}), nonlinear refractive coefficients (n_2), and nonlinear figures of merit (f) for DPC and DBC.

Wavelength/nm	DPC			DBC		
	$\beta_{\text{eff}}/10^{-2}$ cm·GW^{-1}	$n_2/10^{-7}$ cm^2·GW^{-1}	f	$\beta_{\text{eff}}/10^{-2}$ cm·GW^{-1}	$n_2/10^{-7}$ cm^2·GW^{-1}	f
760	4.2	1.8	0.06	3.1	1.4	0.06
800	5.0	4.5	0.11	3.6	3	0.104
850	2.7	4.1	0.14	1	2.4	0.28
900	1.2	4	0.37	0.14	1.8	1.42
950	0.22	3.5	1.67	–	–	–
1000	0.15	3.2	2.13	–	–	–

4. Conclusions

In summary, two materials with a D-π-A structure based on the diphenylacetylene (D) group and the carbaldehyde (A) group were prepared. The response of transient absorption spectra can be modulated by tuning the population of the LE states. Moreover, the RSA and NLO coefficients can also be enhanced under the modulation. Our experimental results show that DPC with a lower population of LE states, due to the extended π-conjugated system, exhibits a wide RSA from visible to near-infrared in transient absorption spectra. Our research on modulating the transient absorption spectra is aimed at guiding the synthesis of broadband NLO materials. The modulation of transient absorption spectra within these types of molecular materials results in fascinating properties, which makes the materials promising candidates in the field of NLO, optical switching, and solar cells.

References

[1] Ehrlich J E, Wu X L, Lee I Y, Hu Z Y, Röckel H, Marder S R and Perry J W 1997 *Opt. Lett.* **22** 1843

[2] He G S, Tan L S, Zheng Q and Prasad P N 2008 *Chem. Rev.* **108** 1245

[3] Almosawe A J and Saadon H L 2013 *Chin. Opt. Lett.* **11** 041902

[4] Si J and Hirao K 2007 *Appl. Phys. Lett.* **91** 091105

[5] Tan W, Liu H, Si J and Hou X 2008 *Appl. Phys. Lett.* **93** 051109

[6] Nguyen V, Si J, Yan L and Hou X 2015 *Carbon* **95** 659

[7] Staub K, Levina G A, Barlow S, Kowalczyk T C, Lackritz H S, Barzoukas M, Fort A and Marder S R 2003 *J. Mater. Chem.* **13** 825

[8] Huang T H, Yang D, Kang Z H, Miao E L, Lu R, Zhou H P, Wang F, Wang G W, Cheng P F, Wang Y H and Zhang H Z 2013 *Opt. Mater.* **35** 467

[9] Achelle S, Barsella A, Caro B and Robin-le Guen F 2015 *RSC Adv.* **5** 39218

[10] Reinhardt B A, Brott L L, Clarson S J, Dillard A G, Bhatt J C, Kannan R, Yuan L X, He G S and Prasad P N 1998 *Chem. Mater.* **10** 1863

[11] Belfield K D, Hagan, D J, Van Stryland E W, Schafer K J and Negres R A 1999 *Org. Lett.* **1** 1575

[12] Antonov L, Kamada K, Ohta K and Kamounah F S 2003 *Phys. Chem. Chem. Phys.* **5** 1193

[13] Polli D, Antognazza M R, Brida D, Lanzani G, Cerullo G and De Silvestri S 2008 *Chem. Phys.* **350** 45

[14] Zewail A H 2000 *J. Phys. Chem. A* **104** 5660

[15] Feng W K, Feng Y Y, Wang S F, Feng W, Yi W H Y and Gong Q H 2010 *Chin. Phys. B* **19** 113401

[16] Lange C, Köster N S, Chatterjee S, Sigg H, Chrastina D, Isella G, von Känel H, Schäfer M, Kira M and Koch S W 2009 *Phys. Rev. B* **79** 201306

[17] Tamaki Y, Furube A, Murai M, Hara K, Katoh R and Tachiya M 2007 *Phys. Chem. Chem. Phys.* **9** 1453

[18] Ruckebusch C, Sliwa M, Pernot P, De Juan A and Tauler R 2012 *J. Photochem. Photobiol. C* **13** 1

[19] Zhou F, Shao J, Yang Y, Zhao J, Guo H, Li X, Ji S, Zhang Z and Zhang Z 2011 *Eur. J. Org. Chem.* **2011** 4773

[20] Haidekker M A, Brady T P, Lichlyter D and Theodorakis E A 2005 *Bioorg. Chem.* **33** 415

[21] Haidekker M A and Theodorakis E A 2007 *Org. Biomol. Chem.* **5** 1669

[22] Stsiapura V I, Maskevich A A, Kuzmitsky V A, Uversky V N, Kuznetsova I M and Turoverov K K 2008 *J. Phys. Chem. B* **112** 15893

[23] Saha S K, Purkayastha P, Das A B and Dhara S 2008 *Photochem. Photobiol A: Chem.* **199** 179
[24] Hwang Y J and Shin D M 2007 *Mol. Cryst. Liq. Cryst.* **472** 25
[25] Klikar M, Bureš F, Pytela O, Mikysek T, Padělková Z, Barsella A, Dorkenoo K and Achelle S 2013 *New J. Chem.* **37** 4230
[26] Wu X, Xiao J, Sun R, Jin T, Yang J, Shi G, Wang Y, Zhang X and Song Y 2017 *Adv. Opt. Mater.* **5** 1600712
[27] Albinsson B, Eng M P, Pettersson K and Winters M U 2007 *Phys. Chem. Chem. Phys.* **9** 5847
[28] Frisch M J, Trucks G W, Schlegel H B, Scuseria G E, Robb M A, Cheeseman J R and Nakatsuji H 2010 Gaussian development version. *Revision h*, 1
[29] Hagberg D P, Marinado T, Karlsson K M, Nonomura K, Qin P, Boschloo G, Brinck T, Hagfeldt A and Sun L 2007 *J. Org. Chem.* **72** 9550
[30] Ajayaghosh A 2003 *Chem. Soc. Rev.* **32** 181
[31] Xia T, Dogariu A, Mansour K, Hagan D J, Said A A, Van Stryland E W and Shi S 1998 *JOSA B* **15** 1497
[32] Ehlers F, Wild D A, Lenzer T and Oum K 2007 *J. Phys. Chem. A* **111** 2257
[33] Liu X, Osgood R M, Vlasov Y A and Green W M 2010 *Nat. Photon.* **4** 557